

# Coherent Quantum Optical Control with Sub-wavelength Resolution

Alexey V. Gorshkov,<sup>1</sup> Liang Jiang,<sup>1</sup> Markus Greiner,<sup>1</sup> Peter Zoller,<sup>2</sup> and Mikhail D. Lukin<sup>1</sup>

<sup>1</sup>*Physics Department, Harvard University, Cambridge, Massachusetts 02138, USA*

<sup>2</sup>*Institute for Quantum Optics and Quantum Information of the Austrian Academy of Sciences, A-6020 Innsbruck, Austria*

(Dated: December 4, 2018)

We suggest a new method for quantum optical control with nanoscale resolution. Our method allows for coherent far-field manipulation of individual quantum systems with spatial selectivity that is not limited by the wavelength of radiation and can, in principle, approach a few nanometers. The selectivity is enabled by the nonlinear atomic response, under the conditions of Electromagnetically Induced Transparency, to a control beam with intensity vanishing at a certain location. Practical performance of this technique and its potential applications to quantum information science with cold atoms, ions, and solid-state qubits are discussed.

PACS numbers:

Coherent optical fields provide a powerful tool for coherent manipulation of a wide variety of quantum systems. Examples range from optical pumping, cooling, and quantum control of isolated atoms [1, 2] and ions [3] to manipulation of individual electronic and nuclear spins in solid state [4, 5]. However, diffraction sets a fraction of the optical wavelength  $\lambda$  as the fundamental limit to the size of the focal spot of light [6]. This prevents one from addressing individual identical atoms if they are separated by a distance of order  $\lambda$  or less. In this Letter, we propose a new method that allows for coherent optical far-field manipulation of quantum systems with resolution that is not limited by the wavelength of radiation and can, in principle, approach a few nanometers.

Our method for coherent sub-wavelength manipulation is based on the nonlinear atomic response produced by so-called dark resonances [7]. The main idea can be understood using the three-state model atom shown in Fig. 1(a). Consider two such atoms, atom 1 and atom 2, positioned along the  $x$ -axis at  $x = 0$  and  $x = d$ , respectively, as shown in Fig. 1(b). Assume that they are prepared in the ground state  $|g\rangle$  and then illuminated by the probe field with wavelength  $\lambda$  and Rabi frequency  $\Omega$ . For  $d \ll \lambda$ , one cannot focus the probe on atom 1 without affecting atom 2 and other neighboring atoms. Let us suppose that  $\Omega$  is uniform over the distance  $d$ . In addition, we apply an auxiliary control field with wavelength  $\lambda'$  and spatially varying Rabi frequency  $\Omega_c(x)$  that vanishes at  $x = 0$  (i.e. has a node). This control field can affect atoms 1 and 2 very differently. Atom 1 will not be affected by the control field since it sits at the point of vanishing intensity, and hence will respond to the probe light in the usual way. At the same time, atom 2 can be completely decoupled from the probe field due to the coherent saturation effect associated with Electromagnetically Induced Transparency [7], provided that control intensity at its position is sufficiently large. The key idea for sub-wavelength addressability is to create the conditions under which the intensity of the control field at the location of atom 2 exceeds that of the probe field,

thereby enabling strongly non-linear response. This is possible no matter how small  $d$  is, provided a sufficiently powerful control field is used.

This selective sub-wavelength addressability can be used in a variety of ways. For example, one can accomplish selective state manipulation of proximally spaced qubits via spatially selective stimulated Raman transitions. In combination with dipole-dipole interactions, our technique can be used to generate an efficient entangling gate between pairs of atoms. One can implement selective fluorescence detection [3] of the internal state of an atom if  $|g\rangle - |e\rangle$  corresponds to a cycling transition (this is possible either if  $|r\rangle$  is above  $|e\rangle$  or if spontaneous emission from  $|e\rangle$  into  $|r\rangle$  is much slower than into  $|g\rangle$ ). Finally, one can perform spatially selective optical pumping of individual atoms. The physical systems, in which we expect these techniques to be particularly useful, include atoms in optical lattices [1], ions in linear Paul traps [3], and optically active defects or quantum dots in solid state [4, 5]. In the remainder of this Letter, we first present a detailed analysis of selective coherent state manipulation and then estimate the manipulation errors using realistic experimental parameters.

Before proceeding, we note important early work. Our approach is an extension of incoherent nonlinear tech-

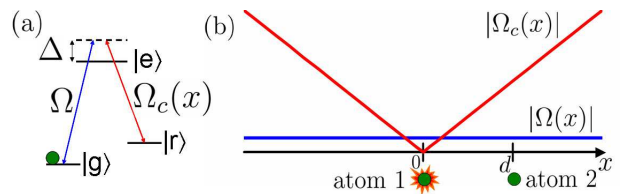


FIG. 1: (color online) (a) 3-level atom prepared in state  $|g\rangle$  and coupled to a spatially uniform probe field with Rabi frequency  $\Omega$  and a spatially varying control field with Rabi frequency  $\Omega_c(x)$ . (b) Schematic of the setup: atom 1 is at a node of the control field and responds to the probe, while atom 2, a distance  $d$  away, is subject to a large control field  $\Omega_c(d) \gg \Omega$  and does not respond to the probe.

niques used in biological imaging [8] and atom lithography [9]. The nonlinear saturation of EIT response that forms the basis of the present work has already been used for the realization of stationary pulses of light [10] and has been suggested for achieving subwavelength localization of an atom in a standing wave ([11, 12] and references therein). Finally, alternative proposals for solving the addressability problem exist that use Bessel probe beams with nodes on all but one atom [13], place atoms into traps separated by more than  $\lambda$  [14], and resolve closely spaced atoms spectroscopically by applying spatially varying magnetic fields [15] or light shifts [16].

As a specific example, we now analyze in detail a spatially selective single-qubit phase gate,  $|0\rangle \rightarrow |0\rangle$ ,  $|1\rangle \rightarrow e^{i\phi}|1\rangle$ , on a qubit encoded in stable atomic states  $|0\rangle$  and  $|1\rangle$  of one atom in the presence of a proximal neighbor (Fig. 2). Consider atoms 1 and 2 that have a tripod configuration shown in Fig. 2(a). By turning on a probe field with Rabi frequency  $\sim \Omega$ , wavelength  $\lambda = 2\pi/k$ , and detuning  $\Delta \gg \Omega$  for a time  $\tau \propto \Delta/\Omega^2$ , we would like to apply a  $\pi$ -phase on state  $|1\rangle$  of qubit 1 via the AC Stark effect. To minimize errors discussed below, we turn  $\Omega$  on and off not abruptly but adiabatically (e.g. a linear ramp up from zero immediately followed by a linear ramp down to zero). To shut off the phase shift on the nearby qubit 2, we apply a spatially varying control field, such as a standing wave, with Rabi frequency  $\Omega_c(x) \approx \Omega_0 k' x$ , where  $k' = 2\pi/\lambda'$  and  $k' x \ll 1$ . We assume the control is turned on before and turned off after the probe pulse. For the moment we consider the idealized situation, in which the atoms are point particles fixed in space, and return to the questions of finite extent of the atomic wave packet (as realized e.g. in a trap) and forces on the atoms below.

The gate error on atom 1 due to spontaneous emission can be estimated as  $\tau\gamma\rho_e \sim \tau\gamma(\Omega/\Delta)^2 \sim \gamma/\Delta$ , where  $\rho_i$  is the population of state  $|i\rangle$  and where we assume for simplicity that all transitions are radiatively broadened and that the decay rate of  $|e\rangle$  is  $2\gamma$ . To investigate the effect on atom 2, we define dark and bright states for this atom as  $|D\rangle = (\Omega_c|1\rangle - \Omega|r\rangle)/\tilde{\Omega}$  and

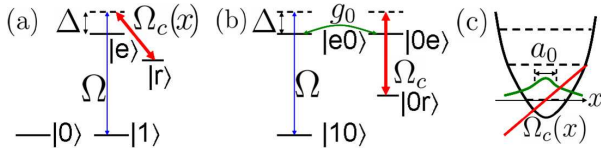


FIG. 2: (color online) Single-qubit phase gate on atom 1. (a) Atom 1 ( $\Omega_c(0) = 0$ ) or atom 2 ( $\Omega_c(d) \neq 0$ ). (b) Two-atom states relevant for understanding the main effect of dipole-dipole coupling ( $|\alpha\beta\rangle$  denotes a two-atom state with atom 1 in  $|\alpha\rangle$  and atom 2 in  $|\beta\rangle$ ) (c) Schematic of imperfect localization of atom 1: parabolic trapping potential  $mw^2x^2/2$  with three lowest energy levels indicated, ground state atomic wavepacket of width  $a_0$ , and control field  $\Omega_c(x) \approx \Omega_0 k' x$ .

$|B\rangle = (\Omega|1\rangle + \Omega_c|r\rangle)/\tilde{\Omega}$ , where  $\tilde{\Omega} = \sqrt{\Omega_c^2 + \Omega^2}$  and  $\Omega_c = \Omega_c(x = d)$ . The phase gate will be turned off iff atom 2 remains in a superposition of  $|0\rangle$  and  $|D\rangle$  without any phase accumulation on  $|D\rangle$  or population loss into  $|B\rangle$ . This will be the case provided the probe field is turned on and off adiabatically as compared with  $|B\rangle$ ,  $|D\rangle$  energy splitting, which is equal to the Stark shift  $\Delta_S = \tilde{\Omega}^2/\Delta$  of  $|B\rangle$ . In the limit  $\Omega_c \gg \Omega$ , which we will assume from now on, the non-adiabatic coupling between  $|D\rangle$  and  $|B\rangle$  has an effective Rabi frequency  $\Omega_{NA} \sim \Omega/(T\Omega_c)$  [17] giving population loss from the dark state into the bright state of order  $\rho_B \sim (\Omega_{NA}/\Delta_S)^2 \sim (\Omega/\Omega_c)^6$  and hence an error of the same order. The errors due to the Stark shift  $\Omega_{NA}^2/\Delta_S$  of  $|D\rangle$  ( $P_e \sim (\Omega_{NA}^2\tau/\Delta_S)^2 \sim (\Omega/\Omega_c)^8$ ) and due to spontaneous emission are smaller than  $(\Omega/\Omega_c)^6$  and  $\gamma/\Delta$ , respectively.

For  $d \ll \lambda$ , dipole-dipole interactions and cooperative decay effects may become important [18]. Cooperative decay will not qualitatively change the errors since the desired evolution is close to unitary. Assuming that we have only two atoms and that  $d \ll \lambda$ , taking the axis of quantization to coincide with the  $x$ -axis, the dipole-dipole Hamiltonian can be written as  $H_{dd} = (\vec{\mu}_1 \cdot \vec{\mu}_2 - 3(\vec{\mu}_1 \cdot \hat{x})(\vec{\mu}_2 \cdot \hat{x}))/d^3$ , where  $\vec{\mu}_i$  is the electric dipole operator of the  $i$ th atom. Since most of the population will stay in  $|0\rangle$  and  $|1\rangle$ , the dipole-dipole interactions involving state  $|r\rangle$  can be ignored. Then provided  $|0\rangle - |e\rangle$  and  $|1\rangle - |e\rangle$  have different polarizations or sufficient frequency difference,  $H_{dd} \approx -g_0(|0e\rangle\langle e0| + |e0\rangle\langle 0e|) - g_1(|1e\rangle\langle e1| + |e1\rangle\langle 1e|)$ , where  $|\alpha\beta\rangle$  denotes a two-atom state with atom 1 in  $|\alpha\rangle$  and atom 2 in  $|\beta\rangle$  and where  $g_0$  and  $g_1$  are proportional to  $g = \gamma/(kd)^3$  with proportionality constants that depend on the polarizations of the transitions. The dominant effect of  $H_{dd}$  can be estimated by supposing that the atoms start in state  $|10\rangle$  and by considering only the 4 states shown in Fig. 2(b) (the error is of the same order for the state  $|11\rangle$ ). A perturbative calculation shows that the dominant effect of  $g_0$  is to reduce the Stark shift of  $|10\rangle$  by a fraction  $\sim (\Omega g/(\Omega_c\Delta))^2$  and to introduce, therefore, an error  $\sim (\Omega g/(\Omega_c\Delta))^4$  [19]. (This error may be reduced in certain cases by slightly adjusting  $\tau$ .) Since  $g$  and, hence, the Stark shift  $V(d)$  are  $d$ -dependent, the application of the phase gate will result in an internal-state-dependent force on the atoms of order  $F \sim \partial_d V(d) \sim \hbar(\Omega g/(\Omega_c\Delta))^2/(\tau d)$ , which can be reduced below the trapping force ( $= mw^2 a_0$  using notation defined below) with a sufficiently powerful control.

Additional errors are associated with imperfections in the control field node and with finite localization of atoms. If atom 1 was perfectly localized at a single point, a residual control field at the node ( $\Omega_c(0) \neq 0$ ) would result in population  $(\Omega_c(0)/\Omega)^2$  in the dark state  $|D\rangle$  (now defined for atom 1). However, even if  $\Omega_c(0) = 0$ , atom 1 can still interact with the control field due to finite extent  $a_0$  of its wave-function. Assuming  $\Omega_c(0) \lesssim \Omega_0 k' a_0$  [20],

1	Error source	Error scaling ( $P_e$ )
1	decay error on atom 1	$\gamma/\Delta$
	<i>localization error on atom 1:</i>	
2	- ions and atoms in fast limit and solid-state qubits	$(\Omega_{ca}/\Omega)^2$
3	- ions and atoms in adiabatic limit	$(\Omega_{ca}/\Omega)^2/(\tau\omega)^4$
4	unitary error on atom 2	$(\Omega/\Omega_c)^6$
5	dipole-dipole error	$(g\Omega/(\Delta\Omega_c))^4$
6	$ r\rangle$ decay on atom 2 for Rb	$(\Omega/\Omega_c)^2\gamma_r\tau$

TABLE I: Error budget.

the error due to finite atomic extent (discussed below) will dominate over  $(\Omega_c(0)/\Omega)^2$ .

To analyze the problem of localization for atoms in optical lattices and ions in linear Paul traps, we assume that atom 1 sits in the ground state of a harmonic oscillator potential with frequency  $\omega$  and, therefore, has spread  $a_0 = \sqrt{\hbar/(2m\omega)}$ , where  $m$  is the mass of the atom, as shown schematically in Fig. 2(c). We assume  $\Omega_c(x) = \Omega_0 k' x = \Omega_{ca}(\hat{a}^\dagger + \hat{a})$ , where  $\Omega_{ca} = \Omega_0(a_0)$  and  $\hat{a}$  is the oscillator annihilation operator.  $\Omega_c(x)$  will then couple  $|e, n\rangle$  and  $|r, m\rangle$  only when  $n = m \pm 1$ , where  $|\alpha, n\rangle$  denotes atom 1 in internal state  $|\alpha\rangle$  in  $n$ th harmonic level. The dominant error can be estimated by keeping only states  $|1, 0\rangle$ ,  $|e, 0\rangle$ , and  $|r, 1\rangle$ . A perturbative calculation shows that the two limits, in which the error is small are: (a) fast limit  $\omega\tau \lesssim 1$ , in which case  $P_e \sim (\Omega_{ca}/\Omega)^2$  (i.e. as if atom 1 were perfectly localized but the control field had value  $\Omega_{ca}$ ); (b) adiabatic limit  $\omega\tau \gg 1$ ,  $(\Omega_{ca}/\Omega)^2$ , in which case a small change in the Stark shift of  $|1, 0\rangle$  can be compensated by slightly adjusting  $\tau$  to yield  $P_e \sim (\Omega_{ca}/\Omega)^2/(\tau\omega)^4$ .

For atom 2 centered at  $x = d$ , we have  $\Omega_c(x) = \Omega_0 k' d + \Omega_c k'(x - d)$ , i.e. the desired coupling  $\Omega_c$  within each harmonic level is accompanied by coupling of strength  $\sim \Omega_{ca}$  between different harmonic levels. Numerical simulations show that provided  $\Omega_{ca} < 0.1 \Omega_c$  (which will always hold below), this coupling has an insignificant effect.

For the case of solid state impurities, we model imperfect localization by replacing  $\Omega_c(0)$  with  $\Omega_{ca} = \Omega_c(a_0)$  to give an error  $\sim (\Omega_{ca}/\Omega)^2$ , where  $a_0$  is the extent of the electronic wavefunction.

The error budget is summarized in Table I. In general, for a given set of experimental parameters, using  $\Omega^2 \sim \Delta/\tau$  to eliminate  $\Omega$  in favor of  $\Delta$ , one has to write the total error as the sum of the errors in Table I and minimize it with respect to  $\Omega_0$  and  $\Delta$  (taking into account possible constraints on their magnitude). We illustrate this procedure for three systems: neutral atoms, ions, and solid-state qubits. We take  $\Omega_{ca} = \Omega_0 k' a_0$ ,  $\Omega_c = \Omega_0$  (except for solid-state qubits, where we take  $\Omega_c = \Omega_0 k' d$ ), and  $\tau = 1 \mu\text{s}$  (except for the Rb example with  $|r\rangle = |4D\rangle$ , where we take  $\tau = 10 \text{ ns}$ ). We note that stimulated Raman transitions [3], resulting in qubit rotations, can also be treated in exactly the same way, yielding similar error

probabilities. Moreover, this error analysis is readily extendable to spatially selective qubit measurements and optical pumping, as well as to dipole-dipole two-qubit gates for proximal atoms.

To analyze atoms in optical lattices, we consider for concreteness  $^{87}\text{Rb}$  with  $|0\rangle = |5S_{1/2}, F = 2, m_F = 2\rangle$ ,  $|1\rangle = |5S_{1/2}, F = 1, m_F = 1\rangle$ , and  $|e\rangle = |5P_{1/2}, F = 2, m_F = 2\rangle$ . Several choices for  $|r\rangle$  exist. For instance,  $|r\rangle = |4D\rangle$  can be used.  $|4D\rangle$  is not metastable and gives an additional error  $\sim \rho_r \gamma_r \tau \sim (\Omega/\Omega_c)^2 \gamma_r \tau$  on atom 2 (error #6 in Table I), where  $2\gamma_r = 1/(90 \text{ ns})$  is the decay rate of  $|4D\rangle$ . To reduce this error, we choose  $\tau = 10 \text{ ns}$ . In Table II, we say whether the error is limited by the magnitude of  $\Omega_0$  (assuming that  $\Omega_0/2\pi = 1 \text{ GHz}$  is the maximum available) and list the parameters used, the errors from Table I that form the dominant balance, and approximate formula and value for the optimal  $\Delta$  and  $P_e$ . Alternatively,  $|r\rangle = |5S_{1/2}, F = 2, m_F = 1\rangle$  can be used. Due to finite hyperfine splitting (6.8 GHz), the strong control field will then introduce an undesired position-dependent Stark shift of  $|1\rangle$ . However, the shift can be compensated by spin-echo type techniques, in which an additional control pulse with proper detuning is applied. The second line in Table II estimates  $P_e$  assuming proper compensation. Further reduction of  $P_e$  is possible if one can ramp up the lattice potential and hence increase  $\omega$  and decrease  $a_0$  for the duration  $\tau$  of the gate.

To analyze ions in linear Paul traps, we consider for concreteness  $^{40}\text{Ca}^+$  [21] with  $|0\rangle = |4S_{1/2}, m = 1/2\rangle$ ,  $|1\rangle = |4S_{1/2}, m = -1/2\rangle$ ,  $|e\rangle = |4P_{1/2}, m = 1/2\rangle$ , and  $|r\rangle = |3D_{3/2}, m = 3/2\rangle$ .  $P_e$  estimate for ions and for solid-state qubits (e.g. Nitrogen-Vacancy color centers in diamond [22]) is made in Table II. For solid-state qubits with  $d < 10 \text{ nm}$ ,  $\Omega_0/2\pi = 1 \text{ GHz}$  is insufficient to suppress the dipole-dipole error (error #5 in Table I), and the gate fidelity sharply drops.

Several approaches to control field node creation are possible. One or two standing waves can be used to generate planes or lines, respectively, of zero field with field amplitudes scaling linearly near the zeros. If one has a regular array of atoms (e.g. in an optical lattice), arrays of zeros can be chosen to have spacing incommensurate or commensurate with atomic spacing, allowing to address single or multiple atoms, respectively. One can also create control field nodes using holographic techniques [23], which allow one to generate single optical vortices (such as in a Laguerre-Gaussian beam) or an arbitrary diffraction-limited two-dimensional array of them. For simplicity, we consider the case when atoms are sensitive only to one polarization of the control field (e.g. if a magnetic field is applied to remove degeneracies). Then the quality of a standing wave node in this polarization component is determined by the interference contrast, which is limited by the mismatch between the amplitudes of this component in the two interfering waves. On the other hand, in an optical vortex, if the phase of

System	$\omega/2\pi$ (MHz)	$a_0$ (nm)	$\lambda$ (nm)	$\lambda'$ (nm)	d (nm)	$\gamma/2\pi$ (MHz)	limited by $\Omega_0$	dominant balance	$\Omega_0/2\pi$ (GHz)	$\Delta$	$\Delta/2\pi$ (GHz)	$P_e$	$P_e$
Rb in an optical lattice	0.3 -    -	14 -    -	795 -    -	1529 795	$\lambda/2$ -    -	3 -    -	no -    -	2 & 6 4 & 2	0.5 0.05	$\Omega_c \Omega_{ca} (\tau/\gamma_r)^{1/2}$ $\Omega_c^2 \tau (k' a_0)^{1/2}$	3 3	$\frac{\Omega_{ca}}{\Omega_c} (\tau \gamma_r)^{1/2}$ $(k' a_0)^{3/2}$	0.04 0.02
Ca <sup>+</sup> in a Paul trap	10	4	397	866	1000	11	yes	4 & 1	1	$(\Omega_c^6 \gamma \tau^3)^{1/4}$	200	$\left(\frac{\gamma}{\tau \Omega_c^2}\right)^{3/4}$	1e-4
solid-state qubit	- -	0.5 -    -	700 -    -	700 20	100 -    -	5 -    -	no -    -	4 & 2 -    -	1 -    -	$\Omega_c^2 \tau \left(\frac{a_0}{d}\right)^{1/2}$	300 25	$\left(\frac{a_0}{d}\right)^{3/2}$ -    -	5e-4 5e-3

TABLE II: Experimental parameters and error estimates for the single-qubit phase gate.

the desired polarization component picks up a nonzero multiple of  $2\pi$  around a closed loop, for topological reasons this loop must enclose a line (in three dimensions) where the amplitude of this polarization component exactly vanishes (see e.g. [24, 25]). Furthermore, the Rabi frequency in an optical vortex rises radially from the center as  $\Omega_c(x) \sim \Omega_0(x/w)^l$ , where  $w \gtrsim \lambda'$  is the beam waist and the topological charge  $l$  is a positive integer. Therefore, in some cases, the use of vortices with  $l > 1$  instead of standing waves or  $l = 1$  vortices can improve the resolution by decreasing the undesired coupling of the control to atom 1. However, since increasing  $l$  requires increasing  $\Omega_0$  to keep  $\Omega_c(d)$  the same, one has to optimize with respect to  $l$  for a given set of experimental parameters.

We now outline some new avenues opened by the coherent selective addressability technique. Although we discussed in detail only the application of this technique to selective phase gates (equivalently, Raman transitions), it has obvious generalizations to geometric gates [26], fluorescence detection, and optical pumping/shelving, as well as to the generation (in combination with dipole-dipole interactions) of entangling gates between atoms. In addition to the applications to atoms in optical lattices, to ions in linear Paul traps, and to solid-state qubits, our technique may also allow for single-atom addressability in recently proposed sub-wavelength optical lattices [27]. Moreover, a combination of similar ideas involving dark states and the nonlinear atomic response can itself be used for creating deep sub-wavelength-separated traps and flat-bottom traps. Finally, better optimization (e.g. using optimal control theory to shape control and probe pulses) can further improve the technique's performance. Therefore, we expect this technique to be of great value for fields ranging from quantum computation and quantum simulation to coherent control, all of which can benefit from high-accuracy sub-wavelength addressability.

We thank D.E. Chang, A. Peng, J. Gillen, T. Calarco, and M.R. Dennis for many fruitful discussions. This work was supported by the NSF, Harvard-MIT CUA, Packard Foundation, and AFOSR MURI. P.Z. acknowledges support by the Austrian Science Foundation and EU grants.

Note added: after completing this work, we became aware of a related proposal [28] to use dark state position dependence to achieve nanoscale microscopy.

- [1] I. Bloch, *Nature Physics* **1**, 23 (2005).
- [2] *Special Issue: Manipulating Coherence*, *Science* **298**, 1353-1377 (2002).
- [3] D. Leibfried *et. al.*, *Rev. Mod. Phys.* **75**, 281 (2003).
- [4] J. Wrachtrup and F. Jelezko, *J. Phys.: Condens. Matter* **18**, S807 (2006).
- [5] M. Atatüre *et. al.*, *Science* **312**, 551 (2006); M. Kroutvar *et. al.*, *Nature* **432**, 81 (2004).
- [6] M. Born and E. Wolf, *Principles of Optics* (Cambridge University Press, Cambridge, England, 1999).
- [7] M. O. Scully and M. S. Zubairy, *Quantum Optics* (Cambridge University Press, Cambridge, England, 1997).
- [8] S. W. Hell, *Nat. Biotechnol.* **21**, 1347 (2003).
- [9] K. S. Johnson *et. al.*, *Science* **280**, 1583 (1998).
- [10] M. Bajcsy, A. S. Zibrov, and M. D. Lukin, *Nature* **426**, 638 (2003).
- [11] M. Sahrai *et. al.*, *Phys. Rev. A* **72**, 013820 (2005).
- [12] G. S. Agarwal and K. T. Kapale, *J. Phys. B: At. Mol. Phys.* **39**, 3437 (2006).
- [13] M. Saffman, *Opt. Lett.* **29**, 1016 (2004).
- [14] S. Bergamini *et. al.*, *J. Opt. Soc. Am. B* **21**, 1889 (2004); Y. Miroshnychenko *et. al.*, *Nature* **442**, 151 (2006).
- [15] D. Schrader *et. al.*, *Phys. Rev. Lett.* **93**, 150501 (2004).
- [16] J. R. Gardner *et. al.*, *Phys. Rev. Lett.* **70**, 3404 (1993); C. Zhang, S. L. Rolston, and S. Das Sarma, *Phys. Rev. A* **74**, 042316 (2006); P. J. Lee *et. al.*, *quant-ph/0702039*.
- [17] M. Fleischhauer and A. S. Manka, *Phys. Rev. A* **54**, 794 (1996).
- [18] J. Guo and J. Cooper, *Phys. Rev. A* **51**, 3128 (1995).
- [19] If  $\Omega_c$  is not sufficiently larger than  $\Omega$ ,  $|0r\rangle$  may accumulate population  $(\Omega g/(\Omega_c \Delta))^2$  to give an error of the same order. However,  $(\Omega g/(\Omega_c \Delta))^2$  and  $(\Omega g/(\Omega_c \Delta))^4$  depend so sharply on  $d$  that they give almost the same resolution.
- [20] The condition is modified in the adiabatic limit (see error #3 in Table I):  $\Omega_c(0) \lesssim \Omega_0 k' a_0 / (\omega \tau)^2$ .
- [21] M. J. McDonnell *et. al.*, *Phys. Rev. Lett.* **93**, 153601 (2004); M. J. McDonnell, D. N. Stacey, and A. M. Steane, *Phys. Rev. A* **70**, 053802 (2004).
- [22] L. Childress *et. al.*, *Science* **314**, 281 (2006); M. V. Gurudev Dutt *et. al.*, *Science* **316**, 1312 (2007).
- [23] J. E. Curtis, B. A. Koss, and D. G. Grier, *Opt. Commun.* **207**, 169 (2002).
- [24] J.F. Nye, *Natural Focusing and Fine Structure of Light*, (Institute of Physics Publishing, Bristol, 1999).
- [25] M.R. Dennis, *New J. Phys.* **5**, 134 (2003).
- [26] L.-M. Duan, J. I. Cirac, and P. Zoller, *Science* **292**, 1695 (2001).

- [27] A. Daley *et. al.* (in preparation).
- [28] D. D. Yavuz and N. A. Proite (in preparation).